Iron stress restricts photosynthetic intersystem electron transport in *Synechococcus* sp. PCC 7942

A.G. Ivanov[a,d], Y.-I. Park[b], E. Miskiewicz[a], J.A. Raven[c], N.P.A. Huner[a], G. Öquist[d,*]

[a] *Department of Plant Sciences, University of Western Ontario, London, Ont., Canada N6A 5B7*
[b] *Department of Biology, Chungnam National University, Taejon 305764, South Korea*
[c] *Department of Biological Science, University of Dundee, Dundee DD1 4HN, UK*
[d] *Department of Plant Physiology, University of Umeå, S-901 87 Umeå, Sweden*

Received 9 September 2000; revised 10 October 2000; accepted 18 October 2000

First published online 7 November 2000

Edited by Richard Cogdell

Abstract Although exposure of *Synechococcus* sp. PCC 7942 to iron stress induced the accumulation of the *isiA* gene product (CP43′) compared with non-stressed controls, immunodetection of the N-terminus of cytochrome (Cyt) *f* indicated that iron stress not only reduced the content of the 40 kDa, heme-binding, Cyt *f* polypeptide by 32% but it also specifically induced the accumulation of a new, 23 kDa, non-heme-binding, putative Cyt *f* polypeptide. Concomitantly, iron stress restricted intersystem electron transport based on the in vivo reduction of $P700^+$, monitored as $\Delta A_{820}/A_{820}$ in the presence and absence of electron transport inhibitors, as well as the inhibition of the Emerson enhancement effect on O_2 evolution. However, iron stress appeared to be associated with enhanced rates of PS I cyclic electron transport, low rates of PS I-driven photoreduction of $NADP^+$ but comparable rates for PS II+PS I photoreduction of $NADP^+$ relative to controls. We hypothesize that *Synechococcus* sp. PCC 7942 exhibits a dynamic capacity to uncouple PS II and PS I electron transport, which may allow for the higher than expected growth rates observed during iron stress.

Key words: Electron transport; Iron stress; Photosystem I; *Synechococcus* sp. PCC 7942

1. Introduction

The photosynthetic apparatus represents one of the most iron-enriched (22 or 23 atoms) cellular systems [2–4], and hence highly vulnerable to iron stress [1,2]. In response to limited iron supply, the number of iron-containing proteins within the photosynthetic apparatus is reduced [3]. Iron stress also inhibits photosystem II (PS II) photochemistry [4], the amount of photooxidizable reaction center pigment of photosystem I (PS I) (P700) [5] and the partial reaction rates associated with PS II and PS I, respectively [3]. Concomitantly, a large decrease in the amount of phycocyanin (Phc) and Chl *a* [3] accompanied by structural alterations of the thylakoid membranes and phycobilisomes [6] as well as a blue shift of 5–6 nm in the main red absorption band of Chl *a* [5] are characteristic of iron-stressed cyanobacteria. The spectral shifts in iron-stressed cells are paralleled by the appearance of a specific iron-stress-induced, *isiA* gene product, the PS II chlorophyll-protein complex, CP43′ [7]. In addition, ferredoxin is replaced by flavodoxin [8]. However, since iron-stressed cyanobacteria remain viable and grow [9,10], we hypothesized that these cells must exhibit a potential to adjust metabolically to low iron conditions. In the present study, we compared the structure, function and composition of the photosynthetic electron transport system of *Synechococcus* sp. PCC 7942 under iron stress and non-stressed conditions in order to elucidate the mechanism by which this cyanobacterium adjusts to low iron conditions.

2. Materials and methods

Synechococcus sp. PCC 7942 cells were grown axenically under non-stress conditions in liquid BG-11 inorganic medium, supplemented with 10 mM 3-[*N*-morpholino]propanesulfonic acid (MOPS) (pH 7.5) and under iron-stress conditions in liquid BG-11 medium lacking Fe-citrate as described earlier [11]. Chl and Phc contents were determined using whole cell spectra according to the method of Myers et al. [12].

Maximal photosynthetic oxygen evolution (P_{max}) and the number of functional PS II centers were measured at 38°C essentially as described earlier [11]. The number of functional PS II centers was calculated by assuming that every functional PS II center produces 1 O_2 molecule for every four flashes [12]. The number of PS I reaction centers was measured from the absorbance changes at 703 nm of thylakoid suspensions as described in [5]. Two separate tungsten light sources providing illumination at 625 nm (light 2) and 675 nm (light 1) (defined by Balzers interference filters) with various intensities were used for the enhancement measurements. Quantitative expression of enhancement was presented according to [13]: $E_2 = (V_{1,2} - V_1)/V_2$, where E_2 is the increase of photosynthetic rate, $V_{1,2}$ is the photosynthetic rate when light 1 and light 2 were presented together whereas V_1 and V_2 are the photosynthetic rates produced independently by light 1 and light 2 respectively.

The redox state of P700 of samples prepared as described by Herbert et al. [14] was determined in vivo using a PAM-101-modulated fluorometer (Heinz Walz GmbH, Effeltrich, Germany) equipped with ED-800T emitter-detector and PAM-102 units following the procedure of Schreiber at al. [15] as described in detail by Ivanov et al. [16]. The redox state of P700 was evaluated as the absorbance change around 820 nm ($\Delta A_{820}/A_{820}$) in a custom-designed cuvette at the

*Corresponding author. Fax: (46)-90-7866676.
E-mail: gunnar.oquist@plantphys.umu.se

Abbreviations: Cyt, cytochrome; DBMIB, 2,5-dibromo-3-methyl-6-isopropyl-*p*-benzoquinone; DCMU, 3-(3,4-dichlorophenyl)-1,1-dimethylurea; DCPIP, 2,6-dichlorophenol-indophenol; FR, far red light; MOPS, 3-[*N*-morpholino]propanesulfonic acid; MT, multiple turnover flash of actinic white light; MV, methyl viologen; P700, reaction center pigment of PS I; $P700^+$, oxidized form of the reaction center of PS I; PC, plastocyanin; PS I, PS II, photosystem I and photosystem II; PQ, plastoquinone; Phc, phycocyanin; P_{max}, maximal photosynthetic oxygen evolution; ST, single turnover flash of actinic white light

0014-5793/00/$20.00
PII: S0014-5793(00)02211-0

growth temperature of 38°C. Stock solutions of electron inhibitors (3 mM 2,5-dibromo-3-methyl-6-isopropyl-*p*-benzoquinone (DBMIB), 1 mM 3-(3,4-dichlorophenyl)-1,1-dimethylurea (DCMU) and 5 mM methyl viologen (MV)) were prepared in 95% (v/v) ethanol. The concentration of ethanol added was always less than 0.5% (v/v).

PS II+PS I-dependent and PS I-dependent photo-reduction of $NADP^+$ in both control (+Fe) and iron-stressed (−Fe) cell cultures of *Synechococcus* sp. PCC 7942 were followed at 340 nm in whole cells according to the procedure of Gerhardt and Trebst [17] as applied by Öquist [5]. Red actinic illumination (>600 nm, 300 μmol photons m^{-2} s^{-1}) was applied for 10 min. Reaction mixture consisted of 10 mM $MgCl_2$, 50 mM Tricine (pH 7.6), 2 mM NADP and cells corresponding to 3 μg Chl ml^{-1}. For PS I-driven NADP-photoreduction assay 10 μM DCMU, 50 μM 2,6-dichlorophenol-indophenol (DCPIP) and 2 mM ascorbate were added. The reaction mixture was prepared under N_2 and maintained anaerobic by an oxygen trap consisting of 10 mM glucose, 13 U ml^{-1} glucose oxidase and 1200 U ml^{-1} catalase [18].

Protein samples containing equal amounts of Chl were separated on 15% (w/v) linear polyacrylamide gels in the presence of 8 M urea and electrophoretically transferred onto nitrocellulose membranes as described earlier [19]. The CP43, CP43′ and cytochrome (Cyt) *f* polypeptides were detected with respective polyclonal antibodies at the following dilutions: CP43, 1:4000; CP43′, 1:4000; Cyt *f*, 1:750. Alternatively, heme-containing polypeptides were detected using enhanced chemiluminescence (Amersham) [20]. Cyt *f*-specific antibodies were generated against a 21 amino acid peptide (H_2N-YPIFAQQGYENPREATGRIVC-COOH) corresponding to the N-terminus of mature Cyt *f* (J.E. Thompson, unpublished results).

3. Results

Growth of *Synechococcus* sp. PCC 7942 cells under iron-stress conditions (−Fe) resulted in a reduction of Chl *a* and Phc content per cell and in a typical iron stress-induced blue shift of 7 nm in the main red Chl *a* absorbance peak [5] compared to control cells (+Fe) (Table 1). Furthermore, the amounts of functional PS II and PS I complexes were also reduced to 64 and 37%, respectively in iron-stressed cells relative to controls. This resulted in almost a doubling in the ratio of PS II/PS I in iron-stressed versus control cultures (Table 1). In addition, immunoblot analysis revealed the appearance of the *isiA* gene product, the CP43′ chlorophyll-binding polypeptide typical for iron-stressed cells [7,9] which was associated with a concomitant 50% decrease in the level of the CP43 polypeptide relative to control cells (Fig. 1A).

Table 1
Characteristics of *Synechococcus* sp. PCC 7942 cells acclimated fully under control, iron sufficient (+Fe) and iron-stressed (−Fe) BG-11 growth medium conditions

Parameter	Medium	
	+Fe	−Fe
μ (h^{-1})	0.033	0.029
Chl *a*	28.9 ± 1.1	16.9 ± 1.0
Phc	22.5 ± 0.5	3.4 ± 0.3
Chl a_{max} (nm)	679	672
PS II	4.4	2.8
PS I	8.3	3.1
PS II/PS I	0.53	0.90
P_{max}	0.35 ± 0.02	0.24 ± 0.01
R	91 ± 11	42 ± 6

Specific growth rates (μ) were determined at the exponential phase of growth. Chl *a* and Phc contents are expressed as relative content per cell density (nmol/A_{750}). Chl a_{max} is the room temperature absorption peak in the red region. Number of functional PS II (mmol PS II/mol Chl) was obtained from repetitive flash O_2 yield measurements. PS I content was measured from the light induced absorbance change at 703 nm. P_{max} – maximal photosynthetic O_2 evolution (mmol O_2 mg Chl^{-1} h^{-1}); *R* – respiration (μmol O_2 consumed mg Chl^{-1} h^{-1}). Mean values were calculated from 5–10 independent experiments.

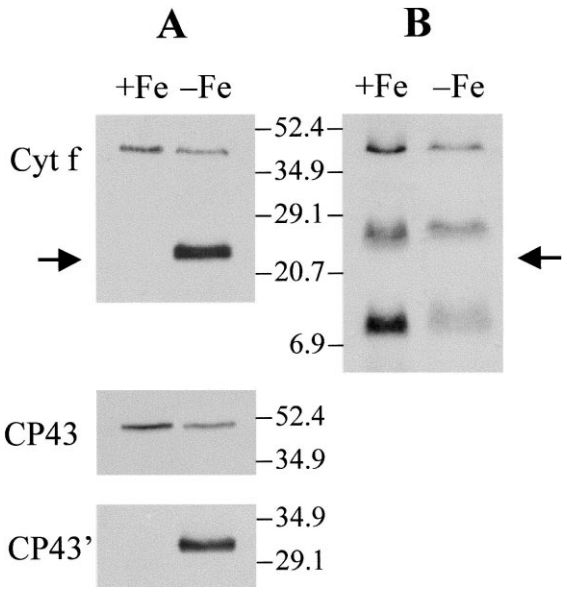

Fig. 1. A: Western blots of SDS–PAGE-separated polypeptides from control, iron sufficient (+Fe) and iron-stressed (−Fe) *Synechococcus* sp. PCC 7942 cells probed with antibodies raised against either the N-terminus of Cyt *f*, CP43, or CP43′. Numbers represent molecular masses of markers. B: Enhanced chemiluminescent heme-staining of SDS–PAGE separated polypeptides from control (+Fe) and iron-stressed (−Fe) cells. Arrow represents a molecular mass of 23 kDa.

In addition, iron-stressed cells not only exhibited a 32% lower level of the 40 kDa Cyt *f* polypeptide than control cells (Fig. 1A) but also exhibited a new 23 kDa polypeptide, which cross-reacted with the Cyt *f*-specific antibodies (Fig. 1A, arrow). Heme-staining of polypeptides from control cells indicated the presence of the 40 kDa Cyt *f* polypeptide as well as the presence of unidentified heme-containing polypeptides of 26 and 10 kDa (Fig. 1B, +Fe). Although polypeptides of the same molecular masses were also detected in iron-stressed cells, the amount of each heme-stained polypeptide was much lower in iron-stressed samples (Fig. 1B, −Fe) than controls. However, the 23 kDa polypeptide observed by immunodetection with the specific Cyt *f* antibody was not detectable by heme staining (Fig. 1B, arrow).

Despite these major alterations in the composition of the photosynthetic apparatus, iron-stressed cells exhibited only a 30% lower P_{max} which was reflected in only a 12% lower growth rate than control cells (Table 1). However, rates of respiration in iron-stressed cells were 50% lower than those of non-stressed, iron-sufficient cells (Table 1).

Estimation of the photooxidizable form of the reaction center of PS I ($P700^+$), measured as $\Delta A_{820}/A_{820}$ [15,21,22], indicated a 4.5-fold lower value for iron-stressed cells relative to control cells (Fig. 2A,D; Table 2). This is consistent with the iron-stress-induced decrease in the amount of functional PS I reaction centers (Table 1). As expected, control cells exhibited a small, rapid oxidation of P700, followed by a transient reduction of $P700^+$ by either PS II and/or cytosolic reductants after the application of single turnover flash of actinic white light (ST) and multiple turnover flashes of actinic white light (MT) (Fig. 2A). In contrast, ST and MT flashes did not in-

duce a transient reduction of $P700^+$ in iron-stressed cells (Fig. 2D).

The lack of any significant DCMU-induced effects on the oxidation level of P700 in both iron-stressed and control cells (Table 2) indicated that PS II did not contribute significantly to the $P700^+$ signal under our conditions of far red light (FR) illumination. Thus, the rate of $P700^+$ re-reduction in the dark is assumed to reflect the rate of cyclic electron flow around PS I [14,16,21]. The observation that the $t_{1/2}$ for the reduction of $P700^+$ is twice as fast in iron-stressed cells as in control cells (Table 2) is indicative of an increased capacity for cyclic electron transport in iron-stressed cells.

To dissect the potential alternative patterns for electron flow to and from PS I, we examined the $P700^+$ transients in the presence of electron transport inhibitors [21]. Blocking the entry of electrons to PS I at the level of Cyt b_6/f complex using DBMIB caused complete oxidation of P700 by FR and decreased the $P700^+$ re-reduction rate in the dark in both controls and iron-stressed cells (Fig. 2C,F; Table 2). Regardless, the $\Delta A_{820}/A_{820}$ remained much lower in iron-stressed than control cells. Furthermore, DBMIB treatment also abolished $P700^+$ reduction after ST and MT flashes indicating that the electron flow from PS II and/or cytosolic sources to $P700^+$ is completely blocked under these conditions.

$HgCl_2$-poisoning of control cells resulted in a 1.8-fold increase in $\Delta A_{820}/A_{820}$ and a 33-fold increase in the $P700^+$ reduction time (Fig. 2B; Table 2). However, the reduction of $P700^+$ after the ST and MT flashes indicates that $HgCl_2$ in control cells did not affect intersystem electron transport in control cells and that PS II must be fully operational under these conditions. In contrast, $HgCl_2$-treated iron-stressed cells exhibited only a 12% increase in $\Delta A_{820}/A_{820}$ and a doubling of the $t_{1/2}$ for $P700^+$ reduction (Fig. 2E; Table 2). Furthermore, ST and MT flashes induced no detectable reduction of $P700^+$ even in $HgCl_2$-treated, iron-stressed cells (Fig. 2E). Since KCN had minimal effects on $\Delta A_{820}/A_{820}$ in either control or iron-stressed cells (Table 2), it is unlikely that a significant leakage of electrons generated by PS II occurs through Cyt oxidase. In both cases, however, the $t_{1/2}$ for the reduction of $P700^+$ increased similarly to those observed in DBMIB-treated samples. The addition of MV caused a further inhibition of the $t_{1/2}$ for $P700^+$ reduction in control and iron-stressed cells indicating that cyclic electron transport around

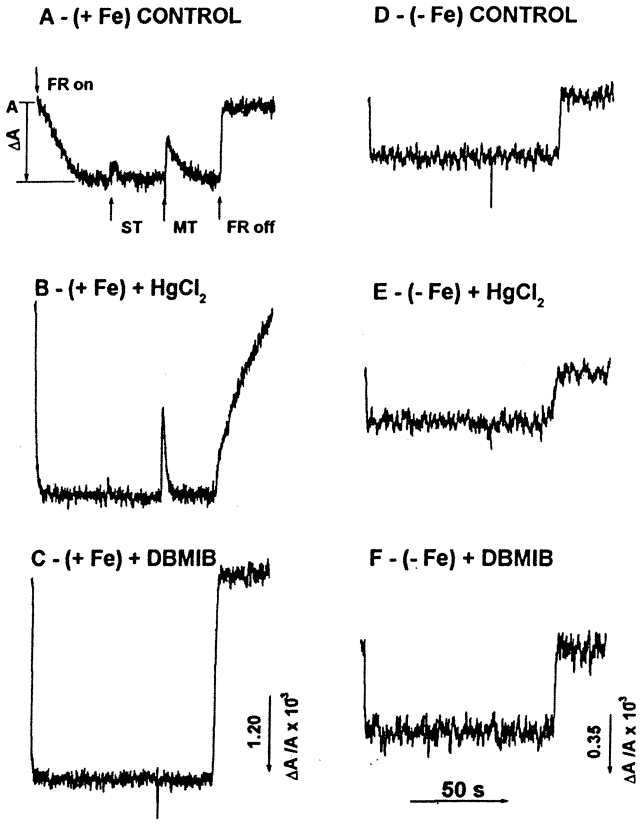

Fig. 2. In vivo measurements of the redox state of P700 in *Synechococcus* sp. PCC 7942 cells grown under control, iron-sufficient (+Fe) and iron-stressed (−Fe) conditions. The measurements were performed at a growth temperature of 38°C as described in Section 2. Data represent typical traces. Samples were prepared on an equal cell number basis of 3×10^6. Experiments were repeated from three to nine times with between 6 and 30 replicate measurements.

PS I is active [21] and that the rate of PS I cyclic transport in iron-stressed cells is still higher than that of control cells (Table 2).

Electron flow between PS II and PS I was also assessed independently by classical photosynthetic enhancement experiments for O_2 evolution [23]. Control cells exhibited an enhancement value (E_2) of about 1.3 for photosynthetic oxygen evolution when exposed to varying ratios of light 1/light 2

Table 2
Effects of iron-stress on the steady state oxidation of P700 ($\Delta A_{820}/A_{820}$) by FR light and half times for $P700^+$ reduction in *Synechococcus* sp. PCC 7942 cells after turning off the FR light

Inhibitor	$\Delta A_{820}/A_{820}$ ($P700^+$) ($\times10^{-3}$)	Re-reduction rate of $P700^+$ $t_{1/2}$ (s)
Control (+Fe)	1.88 ± 0.08	0.402 ± 0.014
+DCMU	2.02 ± 0.17	0.420 ± 0.036
+DCMU+KCN	1.69 ± 0.34	0.590 ± 0.052
+DBMIB	3.51 ± 0.16	0.760 ± 0.038
+$HgCl_2$	3.32 ± 0.18	13.052 ± 1.294
+DCMU+KCN+MV	0.95 ± 0.04	1.314 ± 0.136
Iron deficient (−Fe)	0.42 ± 0.01	0.214 ± 0.013
+DCMU	0.37 ± 0.01	0.252 ± 0.028
+DCMU+KCN	0.37 ± 0.03	0.670 ± 0.150
+DBMIB	0.84 ± 0.06	0.600 ± 0.070
+$HgCl_2$	0.48 ± 0.02	0.513 ± 0.065
+DCMU+KCN+MV	0.35 ± 0.01	1.813 ± 0.203

The final concentrations of inhibitors used were as follows: 10 μM DCMU; 1 mM KCN; 12 μM DBMIB; 100 μM $HgCl_2$; 100 μM MV. These solutions were prepared as described in Section 2. All data represent mean values ± S.E.M. from 6 to 30 measurements in 3–9 independent experiments.

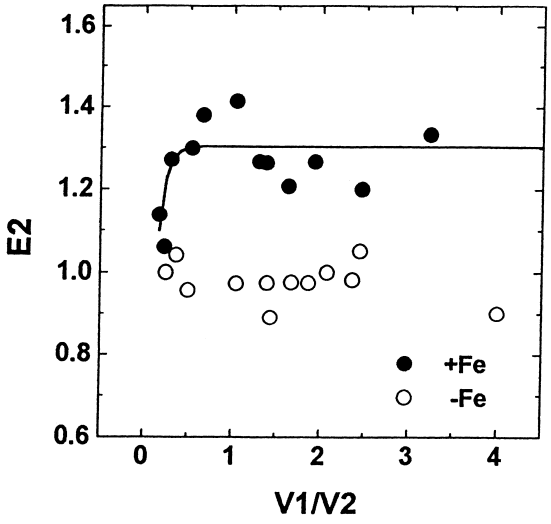

Fig. 3. Enhancement of photosynthetic oxygen evolution as a function of different ratios of V_1/V_2 in *Synechococcus* sp. PCC 7942 cells grown under control (closed circles) or iron-stressed conditions (open circles). Measurements were made as described in Section 2. The data represent averages from three independent experiments.

(Fig. 3). In contrast, we were unable to detect any photosynthetic enhancement in iron-stressed cells (Fig. 3).

The relative impact of PS II and PS I on the photoreduction of $NADP^+$ was estimated in iron-stressed and control cells by measuring ΔA_{340} at the same final Chl concentration. Under conditions whereby both PS II and PS I are fully functional, the ΔA_{340} for $NADP^+$ photoreduction was only 18% lower in iron-stressed cells (0.058 ± 0.007) than controls (0.071 ± 0.006). However, under conditions whereby only PS I is capable of photoreducing $NADP^+$ (+10 μM DCMU, +50 μM DCPIP/2 mM ascorbate), the ΔA_{340} for iron-stressed cells (0.013 ± 0.001) was 65% lower than that of controls (0.037 ± 0.003). Furthermore, these data indicate that inhibition of PS II with DCMU caused a 78% inhibition in ΔA_{340} in iron-stressed cells but only a 48% inhibition in control cells. Thus, it appears that iron-stressed cells are more dependent upon PS II for the photoreduction of $NADP^+$ than control cells.

4. Discussion

Consistent with previous reports for cyanobacteria [4,5,8,9], *Synechococcus* sp. PCC 7942 cells exposed to iron-stress exhibited the expected lower P_{max} for O_2 evolution, a decrease in phycobilisome content, an increase in the PS II/PS I ratio, a blue shift in the Chl *a* absorption maximum and the induction of the *isiA* gene encoding CP43′ (Table 1; Fig. 1). However, we show for the first time that the relative content of the 40 kDa Cyt *f* polypeptide decreased in iron-stressed cells based not only on immunoblots but also based on heme staining (Fig. 1). Furthermore, a new 23 kDa polypeptide accumulated in iron-stressed cells but not control cells (Fig. 2). Since this 23 kDa polypeptide cross-reacted with the specific antibodies raised against the N-terminal region of Cyt *f* but did not bind heme, we suggest that this 23 kDa polypeptide may represent a putative, non-functional form of Cyt *f* induced by iron stress. Furthermore, heme-staining also showed that two other unidentified, heme-containing polypeptides of 26 and 10 kDa were also present at reduced levels in iron-stressed cells. The unidentified hemes probably represent other Cyts involved in photosynthetic and respiratory electron transport. These structural data are consistent with the functional data which indicate, first, that photosynthetic intersystem electron transport was inhibited in iron-stressed versus control cells based on P700 measurements (Fig. 2; Table 2) as well as the Emerson enhancement data (Fig. 3), and second, that the rate of respiration was 50% lower in iron-stressed compared to control cells. However, the minimal decline in the growth rate observed in iron-stressed cells (Table 1) is consistent with earlier reports [9,10] and indicates that the altered composition of the photosynthetic apparatus may reflect, in part, a compensatory mechanism to maintain competitive growth rates under low-iron conditions.

Given that photosynthetic and respiratory electron transfer chains of cyanobacteria share common redox components [24], a number of electron donating systems may supply the plastoquinone (PQ)-pool and Cyt b_6/f complex with electrons. Electron flow originating from either PS II, the NAD(P)H dehydrogenase-mediated stromal electron pathway or cyclic electron pathway(s) around PS I, as well as the consumption of electrons by Cyt oxidase may all contribute to intersystem electron transport and affect PS I photochemistry [14,21]. Thus, the measurement of P700 redox transients in the presence and absence of electron transport inhibitors provides insight into the possible compensatory paths of photosynthetic electron flow in iron-stressed cells compared to control cells. The apparent lower oxidation level of P700 and the altered $t_{1/2}$ for $P700^+$ reduction in iron-stressed cells under FR (Fig. 2; Table 2) could be an indication not only of much lower absolute amount of PS I centers (Table 1) but could also be due to a rapid donation of electrons to $P700^+$ from the cytosolic substrates via the NADH/NAD(P)H dehydrogenase-dependent pathway as proposed previously [21]. The significantly lower P700 photooxidation level in iron-stressed cells even in the presence of $HgCl_2$ (Fig. 2; Table 2) indicates that very few electrons from cytosolic sources appear to be available for the reduction of $P700^+$ through NAD(P)H dehydrogenase under iron-stressed conditions.

The lack of photosynthetic enhancement of O_2 evolution (Fig. 3) together with the results summarized in Fig. 2 and Table 2 indicate that electron transport between PS II and PS I is functionally impaired in iron-stressed cells. Concomitantly, the rate of PS I-dependent cyclic electron transport appears to be increased under iron stress. Conversely, one could argue that the slower photooxidation rate of P700 by FR might be also considered as an indication for higher cyclic electron flux in control than in iron-stressed cells (Fig. 2A,D). In our opinion, however, this is a rather indirect measure of the PS I-dependent cyclic electron flow and the slower oxidation of P700 is more likely to reflect slower oxidation of the much larger (and mostly reduced in darkness) PQ pool in iron sufficient cells. This is supported by the higher respiration rate in iron sufficient cells (Table 1) and the marginal effect of $HgCl_2$ on P700 photooxidation in iron stressed cells (Table 2).

These functional data for a restriction in intersystem electron transport are consistent with the observed decrease in the abundance of the 40 kDa Cyt *f* polypeptide and the concomitant accumulation of a putative, non-functional 23 kDa Cyt *f* polypeptide during iron stress. A similar lack of PS II-dependent re-reduction of P700 was observed in a Cyt b_6/f tobacco

mutant, although the two photosystems were physiologically intact and active [25]. Furthermore, it is established that PS I may be functionally separated from PS II in plants exposed to low temperatures [26] and that nitrogen-fixing cultures of *Plectonema boryanum* exhibit partial uncoupling of photosystems during the diazotrophic phase [27].

In summary, we conclude that, under iron-stress conditions, intersystem electron transport typically associated with linear electron transport [28] is impaired in *Synechococcus* sp. PCC 7942, in part, due to the altered structure and content of Cyt *f*. Based on the impaired capacity of PS II to photoreduce $P700^+$ coupled with a faster $t_{1/2}$ for $P700^+$ reduction in the dark (Fig. 2; Table 2) as well as the apparent lack of photosynthetic enhancement of O_2 evolution (Fig. 3), we suggest that, under iron-stress growth conditions, *Synechococcus* sp. PCC 7942 appears to exhibit a dynamic capacity to uncouple, at least partially, PS II from PS I electron transport as originally suggested by Arnon [29]. However, reasonable growth rates (Table 1) may be maintained because PS I operates predominantly in a cyclic mode generating a proton gradient and ATP, while $NADP^+$ may be photoreduced, at least partially, by PS II. We hypothesize that the observed reorganization of the photosynthetic apparatus may impart a significant advantage for the energy metabolism and growth of *Synechococcus* sp. PCC 7942 exposed to iron stress.

Acknowledgements: This work was financially supported by grants from the Swedish Foundation for International Cooperation in Research and Higher Education (STINT) to G.Ö. and N.P.A.H., the Swedish National Science Research Council to GÖ and the Natural Science and Engineering Research Council of Canada to N.P.A.H. The authors are grateful to Dr. J.E. Thompson, University of Waterloo, for the donation of the Cyt *f* antibody.

References

[1] Raven, J.A., Evans, M.C.W. and Korb, R.E. (1999) Photosynth. Res. 60, 111–149.
[2] Behrenfeld, M.J., Bale, A.J., Kolber, Z.S., Aiken, J. and Falkowski, P.G. (1996) Nature 283, 508–511.
[3] Sandmann, G. (1985) Photosynth. Res. 6, 261–271.
[4] Spiller, S. and Terry, N. (1980) Plant Physiol. 65, 121–125.
[5] Öquist, G. (1974) Physiol. Plant. 30, 30–37.
[6] Sherman, D.M. and Sherman, L.A. (1983) J. Bacteriol. 156, 393–401.
[7] Pakrasi, H.B., Reitham, H.C. and Sherman, L.A. (1985) Proc. Natl. Acad. Sci. USA 82, 6903–6907.
[8] Straus, N.A. (1994) in: The Molecular Biology of Cyanobacteria (Bryant, D.A. Ed.), pp. 731–750, Kluwer Academic, Dordrecht.
[9] Falk, S., Samson, G., Bruce, D., Huner, N.P.A. and Laudenbach, D. (1995) Photosynth. Res. 45, 51–60.
[10] Henley, W.J. and Yin, Y. (1998) J. Phycol. 34, 94–103.
[11] Park, Y.-I., Sandström, S., Gustafsson, P. and Öquist, G. (1999) Mol. Microbiol. 32, 123–129.
[12] Myers, J., Graham, J.R. and Wang, R.T. (1980) Plant Physiol. 66, 1144–1149.
[13] Jones, L.W. and Myers, J. (1964) Plant Physiol. 39, 938–946.
[14] Herbert, S.K., Martin, R.E. and Fork, D.C. (1995) Photosynth. Res. 46, 277–285.
[15] Schreiber, U., Klughammer, C. and Neubauer, C. (1988) Z. Natursorsch. 43c, 686–698.
[16] Ivanov, A.G., Morgan, R.M., Gray, G.R., Velitchkova, M.Y. and Huner, N.P.A. (1998) FEBS Lett. 430, 288–292.
[17] Gerhardt, B. and Trebst, A.Z. (1965) Z. Naturforsch. 20b, 879–885.
[18] Arnon, D.I. and Barber, J. (1990) Proc. Natl. Acad. Sci. USA 87, 5930–5934.
[19] Morgan, R.M., Ivanov, A.G., Priscu, J.C., Maxwell, D.P. and Huner, N.P.A. (1998) Photosynth. Res. 56, 303–314.
[20] Vargus, C., McEwan, A.G. and Downie, J.A. (1993) Anal. Biochem. 209, 323–326.
[21] Mi, H., Endo, T., Schreiber, U., Ogawa, T. and Asada, K. (1992) Plant Cell Physiol. 33, 1233–1237.
[22] Cornic, G., Bukhov, N.G., Wiese, C., Bligny, R. and Heber, U. (2000) Planta 210, 468–477.
[23] Myers, J. (1971) Annu. Rev. Plant Physiol. 22, 289–312.
[24] Scherer, S. (1990) Trends Biochem. Sci. 15, 458–462.
[25] Hager, M., Biehler, K., Illerhaus, J., Ruf, S. and Bock, R. (1999) EMBO J. 18, 5834–5842.
[26] Manuel, N., Cornic, G., Aubert, S., Choler, P., Bligny, R. and Heber, U. (1999) Oecologia 119, 149–158.
[27] Misra, H.S. and Rakesh, T. (1994) Microbiology 140, 971–976.
[28] Hill, R. and Bendall, D.S. (1960) Nature 186, 136–137.
[29] Arnon, D.I. (1995) Photosynth. Res. 46, 47–71.